TASK QUARTERLY 7 No 2 (2003), 243–256

THE STRUCTURE OF Pb–PbO–SiO_2 GLASS VIA MOLECULAR DYNAMICS SIMULATION

JAROSŁAW RYBICKI[1,2], AGNIESZKA WITKOWSKA[1,2], GRZEGORZ BERGMAŃSKI[1], GIORGIO MANCINI[3] AND SANDRO FELIZIANI[3]

[1] *Faculty of Technical Physics and Applied Mathematics, Gdansk University of Technology, Narutowicza 11/12, 80-952 Gdansk, Poland* {*ryba,agnieszk*}*@task.gda.pl*

[2] *TASK Computer Centre, Gdansk University of Technology, Narutowicza 11/12, 80-952 Gdansk, Poland*

[3] *INFM UdR Camerino, Università di Camerino, via Madonna delle Carceri, I-62032 Camerino (MC), Italia giorgio.mancini@unicam.it*

(Received 22 May 2002)

Abstract: The paper is dedicated to a molecular dynamics (MD) study of the structure of partially reduced lead-silicate glass of composition 1Pb 1PbO $1SiO_2$. The simulations have been performed in the constant volume regime, using a two-body potential (Born-Mayer repulsive forces, and Coulomb forces due to full ionic charges). The system was initially prepared as a well equilibrated hot melt, and then slowly cooled down to 300K. The information on short-range correlations were obtained in a conventional way (from pair and angular distribution functions), while the medium-range order was studied via cation-anion ring analysis. In the paper, the short- and medium-range order in the simulated system is discussed and compared with the structure of a glassy completely reduced system, *i.e.* 2Pb $1SiO_2$ and unreduced one, *i.e.* 2PbO $1SiO_2$ glass.

Keywords: lead-silicate glasses, oxide glasses, medium-range order, ring analysis, molecular dynamics simulations

1. Introduction

Lead-silicate glasses find a lot of industrial, mainly optical, applications [1]. As special materials, they are used in electronics and optoelectronics in the production of image plate amplifiers and scintillators [2]. Modified lead-silicate glasses, containing metallic Pb granules, reveal a high secondary emission coefficient, and thus find application in the production of electron channel multipliers [3].

The atomic structure of the lead-silicate glasses has been investigated for sixty years. Various experimental techniques were used, such as IR spectroscopy [4],

Raman spectroscopy [4–6], NMR [5, 7, 8], XPS [9], X-ray diffraction [10, 11], neutron diffraction methods [12, 13], EXAFS (Extended X-ray Absorption Fine Structure) and XANES (X-ray Absorption Near-Edge Structure) [7, 8, 14–17]. Also extensive molecular dynamics (MD) simulations were performed in the whole range of glass-formation [17–23], both for unreduced, and completely reduced lead-silicate systems, *i.e.* for xPbO $(1-x)$$SiO_2$, and xPb $(1-x)$$SiO_2$, $(0.1 \leq x \leq 0.9)$, respectively.

The present contribution is dedicated to a molecular dynamics (MD) [24, 25] study of the structure of a partially reduced lead-silicate glass of composition 1Pb 1PbO 1SiO_2.

The paper is organised as follows. In Section 2 we describe the applied simulation technique, and the data analysis methods. The simulation results are described, discussed and compared with the structures of unreduced and completely reduced systems of analogous stoichiometries in Section 3. Section 4 contains conclusions.

2. Simulation technique and data analysis methods

2.1. MD runs

The molecular dynamics simulations have been performed in the constant volume regime (NVE ensemble). The atoms were assumed to interact by the two-body Born-Mayer-Huggins potential:

$$V_{ij}(r) = \frac{q_i q_j}{4\pi\varepsilon_0 r} + A_{ij}\exp[(\sigma_{ij} - r)/b_{ij}], \tag{1}$$

containing the Born-Mayer repulsive contribution, and Coulomb interactions. We used full ionic charges. The potential parameters A_{ij}, b_{ij} and σ_{ij}, taken from [18], were previously successfully exploited in the (NpT) simulations of the xPbO $(1-x)$$SiO_2$ glasses for $0.1 \leq x \leq 0.9$ [20–23, 17]. The number of atoms within the simulation box with the usual periodic boundary conditions was equal for the 1Pb 1PbO 1SiO_2 glass to 3000 (500 Pb^0, 500 Pb^{2+}, 500 Si^{4+}, and 1500 O^{2-}). The edge of the cubic simulation box amounted to 39.4Å. Dimensions of the 2Pb 1SiO_2 and 2PbO 1SiO_2 samples, considered for the sake of structure comparisons, were similar. The pressure was calculated during the sampling runs from the virial theorem. The sample was initially prepared in a well equilibrated molten state at 10 000K, and cooled at the average rate of $2 \cdot 10^{13}$K/s down to 300K, passing equilibrium states at 8 000K, 6 000K, 5 000K, 4 000K, 3 000K, 2 500K, 2 000K, 1 500K, 1 000K, and 600K. The temperature scaling was applied whenever the rolling average of the temperature (calculated over last 100 time steps) went out of the interval $(T-\Delta T, T+\Delta T)$. At each intermediate temperature the system was being equilibrated during 30 000fs time steps, using $\Delta T = 100$K for $T \geq 1\,000$K, and $\Delta T = 20$K and $\Delta T = 10$K for $T = 600$K and $T = 300$K, respectively. Equilibrated systems were sampled during 10 000fs time steps.

2.2. Structure analysis

The structural information on short-range correlations were obtained in a conventional way, mainly from pair and angular distribution functions (PDFs, and ADFs, respectively). As it has been shown in a number of papers, the PDFs in disordered systems can be decomposed in a short-range peak of a well-defined shape, and a long-range tail [26, 27]. A simple Gaussian shape of the short-range peak of PDF is usually

insufficient to describe accurately the short-range ordering in highly disordered systems. A useful parameterisation of the first PDF peak, as shown in [27, 28], has the form:

$$g(r) = \frac{Np(r)}{4\pi\rho r^2}, \tag{2}$$

where N is the co-ordination number, ρ is the density. The bond length probability density $p(r)$ is described by a Γ-like distribution. The corresponding formula, valid for $(r-R)\beta > -2\sigma$, reads:

$$p(r) = \frac{2}{\sigma\cdot|\beta|\cdot\Gamma(4/\beta^2)}\cdot\left(\frac{4}{\beta^2}+\frac{2(r-R)}{\sigma\cdot\beta}\right)^{\frac{4}{\beta^2}-1}\cdot\exp\left[-\left(\frac{4}{\beta^2}+\frac{2(r-R)}{\sigma\cdot\beta}\right)\right]. \tag{3}$$

Here R is the average distance, σ^2 is the variance (Debye-Waller-like parameter), β is the asymmetry (skewness) parameter, and $\Gamma(x)$ is the Euler's gamma function.

In order to describe the second, and further co-ordination shells, *i.e.* to describe the medium-range order, instead of analysing the PDFs and ADFs, one should use more advanced methods of the structural analysis. One of the possible approaches consists in the analysis of properly constructed clusters of edge and/or face sharing Voronoï polyhedra [29–31]. This method, although very efficient in the detection of crystalline regions of various symmetry [32] works well for close packed systems. In open systems serious problems appear in the construction of the Voronoï network, and in the procedures eliminating short edges and small faces. In such cases, the cation-anion ring analysis seems to be an ideal tool for characterising the medium-range order. The medium-range order was studied mainly via cation-anion ring analysis, performed using a new highly efficient redundancy aware algorithm. The algorithm is based on the communication network simulation proposed for an efficient exact solution of the Ring Perception Problem [33]. However, a new approach named "pre-filtering" technique [34, 35] has been recently developed to perceive rings in structures represented by 2-connected graphs. Our approach enforces full rings formation (*i.e.* a ring of length n is assured to close on each of its n nodes leading to n equal rings), so that, once detected and processed for linear independence all n-sized rings closing on a node N, all n-sized rings closing on a different node M, and including node N, can be safely regarded, and ignored as copies of rings previously processed. The structure of the determined basal rings was investigated using the ANELLI programme package [36–38].

3. Results and discussion

The short-range ordering around the Si^{4+} and Pb^{2+} cations is described in Subsections 3.1 and 3.2, respectively. In Subsection 3.3 we discuss the medium-range order in the ionic subsystem, whereas the behaviour of neutral Pb^0 subsystem is presented in Subsection 3.4.

3.1. Short-range order around silicon ions

The first Si^{4+}–O^{2-} PDF peak in 1Pb 1PbO 1SiO_2 is very symmetric (Figure 1a). The best-fit parameters of Equations (2)–(3), R, σ^2, β, and N are listed in Table 1. The table contains also the PDFs' maxima positions, *i.e.* the most probable interatomic distances, R_o. As reported in Table 1, the most probable Si^{4+}–O^{2-} distance,

R_o, and the mean Si^{4+}–O^{2-} distance, R, both equal to 1.64 Å. The cited values are somewhat lower than in completely reduces glass, 2Pb $1SiO_2$, and somewhat higher than in unreduced glass, 2PbO $1SiO_2$. The Si^{4+}–O^{2-} distances have been measured experimentally only for the unreduced 2PbO $1SiO_2$ glass, giving 1.6 Å [10], 1.62 Å [11], and 1.63 Å [12]. The latter values are compatible with our MD result (*cf.* Table 1). Our simulations predict systematic increase of the Si^{4+}–O^{2-} distance with increasing reduction degree.

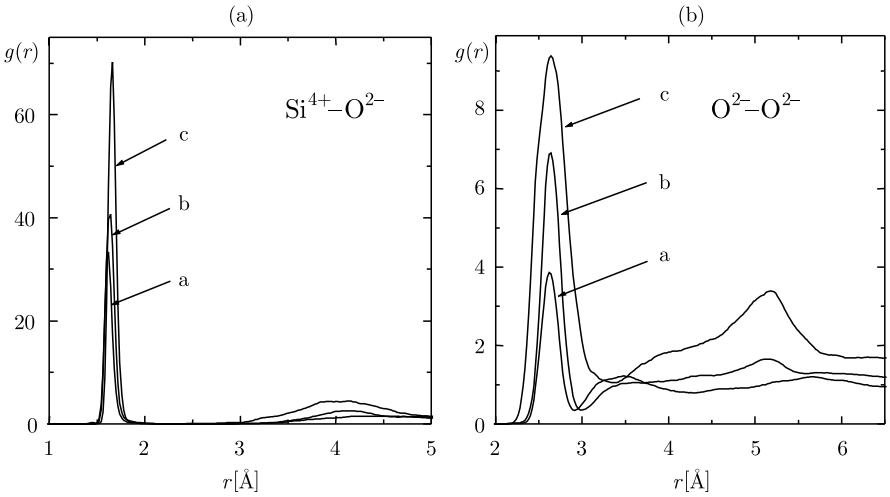

Figure 1. Si^{4+}–O^{2-} (Figure a) and O^{2-}–O^{2-} (Figure b) partial pair distribution functions in 2Pb $1SiO_2$ (curves a), 1Pb 1PbO $1SiO_2$ (curves b) and 2PbO $1SiO_2$ (curves c) glasses

Table 1. Parameters of the first Si^{4+}–O^{2-} peak in the 2Pb $1SiO_2$, 1Pb 1PbO $1SiO_2$ and 2PbO $1SiO_2$ glasses

Si^{4+}–O^{2-} first RDF's peak	R_0 [Å]	R [Å]	σ^2 [Å^2]	β	N
2Pb $1SiO_2$	1.66	1.66	0.0017	0.3	3.93
1Pb 1PbO $1SiO_2$	1.64	1.64	0.0022	0.2	3.94
2PbO $1SiO_2$	1.62	1.63	0.0019	0.5	3.90

The average Si^{4+}–O^{2-} co-ordination numbers, determined using a Γ-function approximation of the first peaks, amount to about 3.9 in all the considered glasses (*cf.* [10], where the value of 3.8 is cited for 2PbO $1SiO_2$).

The most probable O^{2-}–O^{2-} distance, R_o, increases systematically with increasing reduction degree, from 2.62 Å for 2PbO $1SiO_2$ to 2.64 Å for 2Pb $1SiO_2$ (Table 2). Simultaneously, the corresponding R values change from 2.64 Å to 2.71 Å. The increase of the O^{2-}–O^{2-} inter-atomic distances with increasing reduction degree is accompanied by the increase of the peak width and its asymmetry (see Table 2 and Figure 1b). The dispersion of the O^{2-}–O^{2-} distances is much wider than of the Si^{4+}–O^{2-} distances: the σ^2 parameter is about 5 times higher for the O^{2-}–O^{2-} correlation than for the Si^{4+}–O^{2-} correlation in 2PbO $1SiO_2$, and about 20 times higher in 2Pb $1SiO_2$. The increase of the mean O^{2-}–O^{2-} distance R and increase of the σ^2 and β parameters with in-

Table 2. Parameters of the first O^{2-}–O^{2-} peak in the 2Pb $1SiO_2$, 1Pb 1PbO $1SiO_2$ and 2PbO $1SiO_2$ glasses

O^{2-}–O^{2-} first RDF's peak	R_0 [Å]	R [Å]	σ^2 [Å^2]	β	N
2Pb $1SiO_2$	2.64	2.71	0.039	0.55	6.3
1Pb 1PbO $1SiO_2$	2.63	2.66	0.012	0.30	4.1
2PbO $1SiO^2$	2.62	2.64	0.011	0.23	3.1

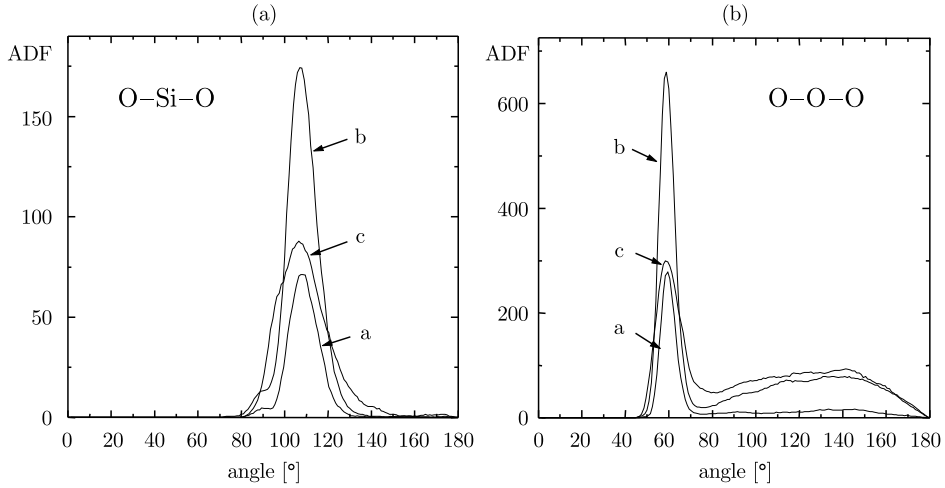

Figure 2. O^{2-}–Si^{4+}–O^{2-} (Figure A) and O^{2-}–O^{2-}–O^{2-} (Figure B) angular distribution functions in 2Pb $1SiO_2$ (curves a), 1Pb 1PbO $1SiO_2$ (curves b) and 2PbO $1SiO_2$ (curves c) glasses

creasing reduction degree is accompanied by an increase of the average co-ordination number: from about 3.1 for 2PbO $1SiO_2$ to about 6.3 for 2Pb $1SiO_2$.

Using the data on inter-atomic distances listed in Tables 1 and 2, and angle distributions from Figure 2, one can conclude, that the SiO_4 tetrahedra are the basic structural units of the silica subsystem. In order to characterise the SiO_4 tetrahedra we used the following tetrahedricity parameters, T_1 [39], and T_2:

$$T_1 = \frac{\sum_i (l_{\mathrm{O-O}} - l_{\mathrm{O-O},i})^2}{l^2_{\mathrm{O-O}}}, \tag{4}$$

$$T_2 = \frac{\sum_i (l_{\mathrm{O-O}} - l_{\mathrm{O-O},i})^2}{l^2_{\mathrm{O-O}}} + \frac{\sum_i (l_{\mathrm{Si-O}} - l_{\mathrm{Si-O},i})^2}{l^2_{\mathrm{Si-O}}}, \tag{5}$$

where $l_{\mathrm{O-O},i}$ and $l_{\mathrm{Si-O},i}$ are the lengths of the i^{th} tetrahedrons' O^{2-}–O^{2-} edge and Si^{4+}–O^{2-} distance, respectively, and $l_{\mathrm{O-O}}$ and $l_{\mathrm{Si-O}}$ are the average O^{2-}–O^{2-}, and Si^{4+}–O^{2-} distances, respectively. The T_1 parameter (4) estimates only the overall shape of the tetrahedra, with no reference to the position of central cation. The T_2 parameter (5) additionally takes into account deviations in the cation localisation. The ideal tetrahedron is characterised by zero-values of both estimators, $T_1 = T_2 = 0$.

The distributions of the values of the tetrahedricity parameters T_1 and T_2 (Table 3) indicate that the tetrahedra in partially reduced 1Pb 1PbO $1SiO_2$ glass are very regular. The maximum values of T_1 and T_2 do not exceed 0.05. 30% and

Table 3. Occurrence [%] of the T_1 and T_2 values for SiO_4 structural units in subsequent bins of width 0.01 in the 2Pb $1SiO_2$, 1Pb 1PbO $1SiO_2$ and 2PbO $1SiO_2$ glasses

Occurrence of T_1 (T_2) values [%]	0.0–0.01	0.01–0.02	0.02–0.03	0.03–0.04	0.04–0.05	0.05–0.06	>0.06
2Pb $1SiO_2$	11 (6)	30 (30)	20 (21)	18 (18)	9.5 (11)	5.5 (5)	6 (9)
1Pb 1PbO $1SiO_2$	66 (48)	29 (44)	3 (6)	1 (2)	1 (2)	— (—)	— (—)
2PbO $1SiO_2$	63 (48)	30 (39)	5 (9)	2 (2.5)	0 (1.5)	— (—)	— (—)

14% of the tetrahedra has the values of T_1 and T_2, lower than 0.005, respectively. The T_1 and T_2 values are lower than 0.02 for 95% and 92% of all the SiO_4 groups, respectively. The above characteristics of the SiO_2 tetrahedra in 1Pb 1PbO $1SiO_2$ glass are very close (1% differences) to those referring to unreduced 2PbO $1SiO_2$ glass, so a 50%-reduction practically does not influence the regularity of the silica basic structural units. However, in completely reduced glass, 2Pb $1SiO_2$, the SiO_4 tetrahedra are much more distorted.

3.2. Short-range order around lead ions

The most probable and the mean Pb^{2+}–O^{2-} distances (R_o and R, respectively) as well as the σ^2 and β parameters do not depend within the determination error with the reduction degree (Figure 3a). Note that the Pb^{2+}–O^{2-} distances obtained in our simulations are by about 0.1 Å longer than reported in [10] (2.25 Å). On the other hand, the average Pb^{2+}–O^{2-} co-ordination numbers depend significantly with progressing reduction: about 5 in 2PbO $1SiO_2$, and about 4.4 in 1Pb 1PbO $1SiO_2$. Note that the latter value is close to the Pb^{2+}–O^{2-} co-ordination in the 1PbO $1SiO_2$ glass, *i.e.* in the glass of the same molar ratio of PbO and SiO_2.

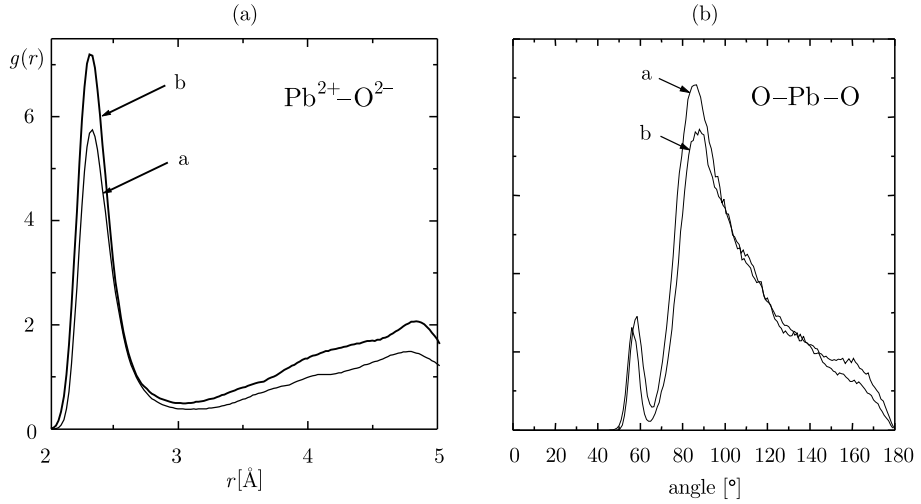

Figure 3. Pb^{2+}–O^{2-} pair correlations and O^{2-}–Pb^{2+}–O^{2-} angle distributions in 1Pb 1PbO $1SiO_2$ (curve a) and 2PbO $1SiO_2$ (curve b) glasses

The distribution of the co-ordination numbers, calculated within the cut-off radius of 3.0 Å, is given in Table 4. As it is seen, in partially reduced glass the

Table 4. Distribution of the Pb^{2+}–O^{2-} co-ordination numbers in 1Pb 1PbO 1SiO_2 and 2PbO 1SiO_2 glasses; the neighbour-search radius was set to 3 Å

Pb^{2+}–O^{2-} co-ordination	3	4	5	6	7
1Pb 1PbO 1SiO_2	13.4%	49.1%	31.3%	5.2%	0.8%
2PbO 1SiO_2	2.8%	38.6%	46.2%	11.4%	1.0%

distribution is narrower than in the unreduced glass. The dominating co-ordinations are equal to 4, and 5, respectively.

Let us discuss the structure of the $Pb^{2+}O^{2-}{}_4$ units. Such units can be divided into two groups: pyramid-like structures (all four neighbours lay in one half-space) and tetrahedron-like structures (the neighbours do not lay in one half-space, and surround the lead ion).

In order to characterise the $Pb^{2+}O^{2-}{}_4$ groups of pyramid-like symmetry (about 30%, and 25% of all the $Pb^{2+}O^{2-}{}_4$ groups in the 2PbO 1SiO_2 and 1Pb 1PbO 1SiO_2, respectively), a shape estimator, P, defined as:

$$P = \frac{\sum_i (l_{\mathrm{Pb-O}} - l_{\mathrm{Pb-O},i})^2}{l^2_{\mathrm{Pb-O}}} + \frac{\sum_i (l_{\mathrm{O-O}} - l_{\mathrm{O-O},i})^2}{l^2_{\mathrm{O-O}}}, \tag{6}$$

has been introduced. In Equation (6) $l_{\mathrm{Pb-O},i}$ is the length of the i^{th} Pb^{2+}–O^{2-} edge, and $l_{\mathrm{Pb-O}}$ is the average length of the Pb^{2+}–O^{2-} edges. Similarly, $l_{\mathrm{O-O},i}$ is the length of the i^{th} O^{2-}–O^{2-} edge, and $l_{\mathrm{O-O}}$ is the average length of the O^{2-}–O^{2-} edges. The distribution of the P values for pyramid-like $Pb^{2+}O^{2-}{}_4$ groups is given in Table 5. As it is seen, the P values of the $Pb^{2+}O^{2-}{}_4$ pyramids have wider and more uniform distribution in 1Pb 1PbO 1SiO_2 than in 2PbO 1SiO_2. Thus, the pyramids are more distorted in partially reduced glass than in unreduced one.

Table 5. Distribution of the piramidicity parameter P of pyramid-like groups $Pb^{2+}O^{2-}{}_4$ in 1Pb 1PbO 1SiO_2 and 2PbO 1SiO_2 glasses

P – range	0.0–0.1	0.1–0.2	0.2–0.3	0.3–0.4	0.4–0.5	0.5–0.6	>0.6
1Pb 1PbO 1SiO_2	39.0%	24.0%	18.0%	10.0%	0.0%	0.0%	3.0%
2PbO 1SiO_2	42.0%	30.0%	12.0%	7.0%	5.0%	2.0%	2.0%

The $Pb^{2+}O^{2-}{}_4$ groups of tetrahedral symmetry constitute about 70%, and 75% of all the $Pb^{2+}O^{2-}{}_4$ groups in the 2PbO 1SiO_2 and 1Pb 1PbO 1SiO_2, respectively. From inspection of the distributions of the T_1 and T_2 parameters it follows, that in contrast to the pyramid-like units, the $Pb^{2+}O^{2-}{}_4$ tetrahedra are more regular in the 1Pb 1PbO 1SiO_2 glass than in the 2PbO 1SiO_2 glass (Table 6).

The $Pb^{2+}O^{2-}{}_5$ and $Pb^{2+}O^{2-}{}_6$ groups, of occurrence frequency given in Table 4, have been identified as distorted triangular and square bi-pyramids, respectively.

3.3. Medium-range order in ionic subsystem

The medium range order can be investigated to some extend by analysing the second-neighbour correlations, in the present case the Si^{4+}–Si^{4+}, and Pb^{2+}–Pb^{2+} PDFs. However, it is usually difficult to arrive to univocal conclusions. Thus, we have

Table 6. Distributions of the tetrahedricity parameters T_1 and T_2 for $Pb^{2+}O^{2-}{}_4$ groups of tetrahedral symmetry in 1Pb 1PbO $1SiO_2$ and 2PbO $1SiO_2$ glasses

	1Pb 1PbO $1SiO_2$	2PbO $1SiO_2$
T_1 (T_2) range	T_1 (T_2) [%]	T_1 (T_2) [%]
0.0–0.05	15.4 (9.2)	8.5 (6.2)
0.05–0.10	46.7 (45.6)	38.0 (34.1)
0.10–0.15	24.1 (25.6)	25.6 (27.1)
0.15–0.2	7.7 (9.7)	14.0 (14.7)
0.20–0.25	1.5 (4.6)	4.7 (7.0)
0.25–0.3	1.5 (1.0)	4.7 (4.7)
>0.3	3.7 (4.1)	4.7 (6.2)

chosen the ring analysis [36–38], that provides a quantitative characterisation of the medium-range order. The ring analysis has been performed as follows.

At first, the full neighbours' list (FNL) for all the atoms of given kinds (*i.e.* Si and O, and Pb and O), were constructed, according to a simple adjacency criterion (user-defined cut-off radius), and taking into account the periodic boundary conditions. The FNL defines a graph, which represents atoms and inter-atomic bonds. In general, the obtained graph does not need to be connected. Thus before further data analysis the full bonding graph was split into separate connected sub-graphs. In order to minimise the execution time and the memory request from the main programme (ring calculation), all the dangling structures were eliminated from the adjacency sub-graphs, *i.e.* all the atoms which do not belong to any ring or path between rings. Then, the ring basis was determined for each connected graph using our algorithm mentioned in Section 2. As the result we obtained full information on basal rings (expressed as the lists of node numbers), and ring length statistic. The concrete set of basal (linearly independent) rings for a given graph depends only on the node enumeration (the base is not unique), but the length distribution is of course unique. A closed chain of bonded atoms, consisting of N cations and N anions, is called an N-member ring [40, 41]. We say that its length equals to N.

Let us discuss in turn the length distributions of the basal Si^{4+}–O^{2-}–Si^{4+}–O^{2-}–… and Pb^{2+}–O^{2-}–Pb^{2+}–O^{2-}–… rings.

Figure 4 shows the distribution of Si^{4+}–O^{2-}–Si^{4+}–O^{2-}–… ring lengths in 2PbO $1SiO_2$, 1Pb 1PbO $1SiO_2$ and 2Pb $1SiO_2$ systems. 5-member rings are dominating in all the samples. In unreduced glass some 2-member silicon-oxygen rings (edge sharing tetrahedra) appear. Such rings are practically absent in reduced (both partially and completely) glasses. Moreover, the percentage of long rings decreases on increasing reduction degree. This means that in reduced samples the silica subsystem is more compact (see Section 3.4).

The distribution of the Pb^{2+}–O^{2-}–Pb^{2+}–O^{2-}–… rings is shown in Figure 5. In a partially reduced glass, 1Pb 1PbO $1SiO_2$, similarly as in unreduced 2PbO $1SiO_2$ glass, the 2-member rings are clearly dominating. In the former case the contribution of longer rings is lower, and the 2-member rings are more frequent than in the unreduced glass.

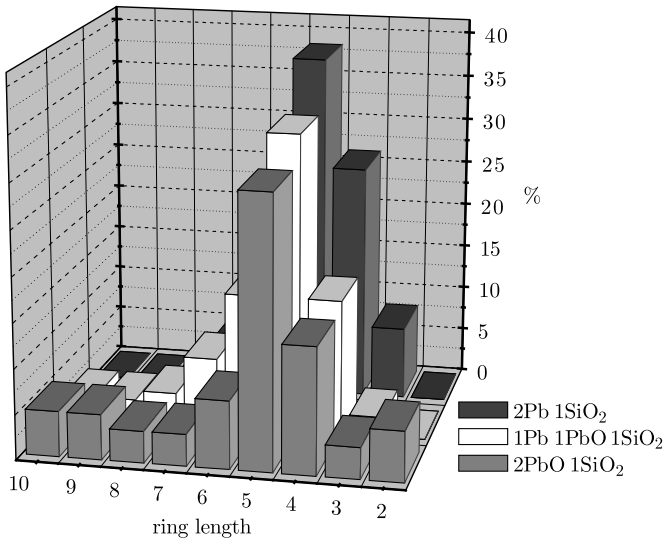

Figure 4. Comparison of the Si^{4+}–O^{2-}–Si^{4+}–O^{2-}–... ring length distributions in 2Pb $1SiO_2$, 1Pb 1PbO $1SiO_2$ and 2PbO $1SiO_2$ glasses

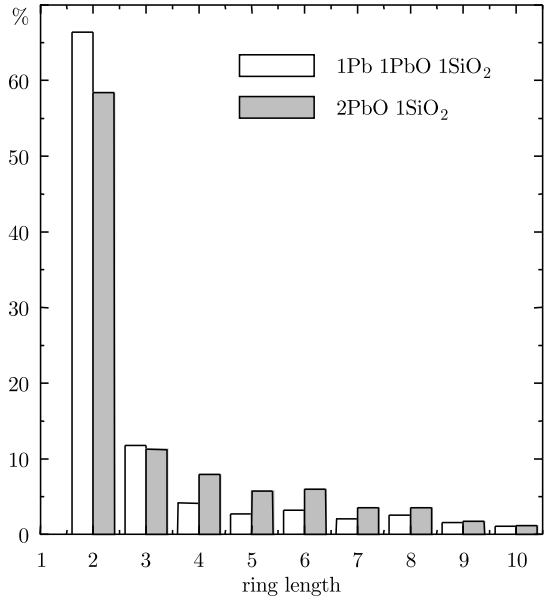

Figure 5. Comparison of the Pb^{2+}–O^{2-}–Pb^{2+}–O^{2-}–... ring length distributions in 1Pb 1PbO $1SiO_2$ and 2PbO $1SiO_2$ glasses

From the analysis of the dominating 2-member Pb^{2+}–O^{2-} rings it results that the $Pb^{2+}O^{2-}{}_4$ units share their O^{2-}–O^{2-} edges. The angular distribution functions for O^{2-}–Pb^{2+}–O^{2-}, and Pb^{2+}–O^{2-}–Pb^{2+} triples calculated over dominating 2-member rings are shown in Figure 6. As it is seen, the O^{2-}–Pb^{2+}–O^{2-} and Pb^{2+}–O^{2-}–Pb^{2+} angle distributions are similar for both 1Pb 1PbO $1SiO_2$ (Figure 6a) and 2PbO $1SiO_2$ (Figure 6b) glasses, and peaked in the range 75°–95°. All the distributions are rather wide, and somewhat shifted one from the other: the Pb^{2+}–O^{2-}–Pb^{2+} angles

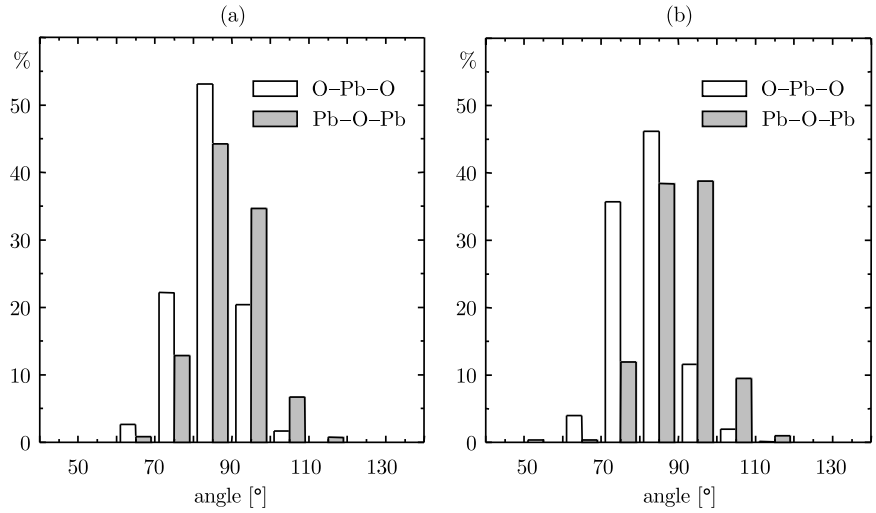

Figure 6. Distributions of the O^{2-}–Pb^{2+}–O^{2-} and Pb^{2+}–O^{2-}–Pb^{2+} angles along 2-member lead-oxygen rings in 1Pb 1PbO $1SiO_2$ (Figure a) and 2PbO $1SiO_2$ (Figure b) glasses

are slightly wider than the O^{2-}–Pb^{2+}–O^{2-} angles (Figure 6). This shift for partially reduced glass is lower than the unreduced glass. However, the distribution of sums of the inter-bond angles along the 2-member rings is sharply peaked between 355° and 360° for both 1Pb 1PbO $1SiO_2$ and 2PbO $1SiO_2$ systems. The distances between the middles of the Pb^{2+}–Pb^{2+} and O^{2-}–O^{2-} diagonals do not exceed 0.5 Å, so the 2-member lead-oxygen rings are rather flat. This means, that the shape of 2-member lead-oxygen rings, characteristic for the mutual configuration of adjacent edge sharing PbO_4 pyramids [42] in crystalline red PbO (P4/nmm space group), is rather well preserved in lead-silicate glasses.

It should be noted that due to the periodic boundary conditions several artefact long rings were detected in each of the samples. These were identified and disregarded in the analysis, so the data shown in Figure 4 and 5 are free of the influence of the periodic boundary conditions.

3.4. Neutral Pb

Figure 7 shows the difference between the Pb^{2+}–O^{2-}, and Pb^{0}–O^{2-} partial pair distribution functions in the 1Pb 1PbO $1SiO_2$ glass. Obviously, because of the Coulomb attraction, the most probable Pb^{2+}–O^{2-} distance (2.33 Å) is much shorter the most probable Pb^{0}–O^{2-} distance (3.72 Å). The latter pair correlation (curve b in Figure 7) is rather untypical. The maximum value in the first peak is lower than one, and the curve reaches the continuum value of one only at about $r = 10$ Å. Such a behaviour of the average PDF means that very few Pb^{0} atoms have oxygen atoms as the first neighbours.

The results described above suggest that both in partially and completely reduced [22] glasses an agglomeration of the Pb^{0} atoms takes place. The agglomeration effect is readily seen via direct visualisation of the atom configuration. In Figure 8 we show the spatial distributions of neutral lead atoms that have Pb^{0}-co-ordination higher than n, $n = 2$, 6, and 12. As it is seen the Pb^{0} atoms in both partially, and com-

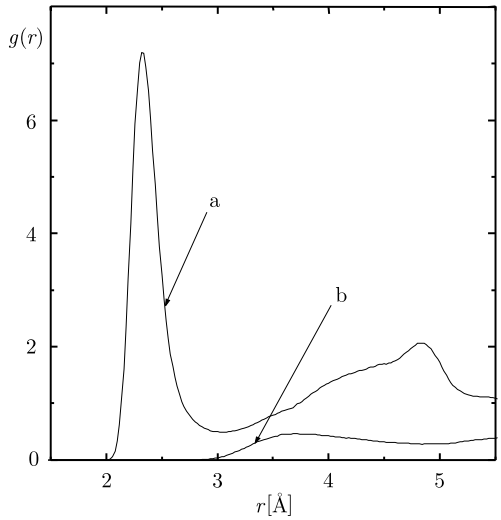

Figure 7. Comparison between the Pb^{2+}–O^{2-} (curve a), and Pb^{0}–O^{2-} (curve b) pair distribution functions in the 1Pb 1PbO $1SiO_2$ glass

pletely reduced samples form single granules (note the effect of the periodic boundary conditions). The fractions of neutral lead atoms that have auto-co-ordination equal or higher than 12 (fully bulk atoms of the granules) amount to about 30% for both samples. Because of limited number of Pb^0 atoms within the simulation boxes (500 for 1Pb 1PbO $1SiO_2$, and 800 for 2Pb $1SiO_2$) one can not extract any size-independent conclusions on typical granule sizes in both systems.

4. Conclusions

The results can be summarised as follows:

- partial reduction (up to 50%-neutralisation of all lead atoms) does not significantly influence the regularity of the tetrahedral SiO_4 structural unit. In completely reduced glass, however, the fraction of more deformed SiO_4 tetrahedra increases;
- with increasing reduction degree the silica subsystem becomes more and more compact: long rings disappear, the contribution of 5-, 6-, and 7-member silicon-oxygen rings, characteristic of pure silica structure, increases;
- partial reduction does not influence significantly the nearest neighbourhood of the Pb^{2+} ions. Both pyramidal and tetrahedral environments coexist, and on increasing reduction the pyramids become somewhat more deformed, whereas the tetrahedra become more regular. In partially reduced glass the fraction of lead ions of co-ordination higher than 4 is lower than in unreduced glass;
- 2-member lead-oxygen rings, characteristic for the mutual configuration of adjacent edge sharing PbO_4 pyramids in crystalline red PbO appear also in the glasses, independently of the reduction degree;
- neutral lead atoms agglomerate into granules independently of the reduction degree.

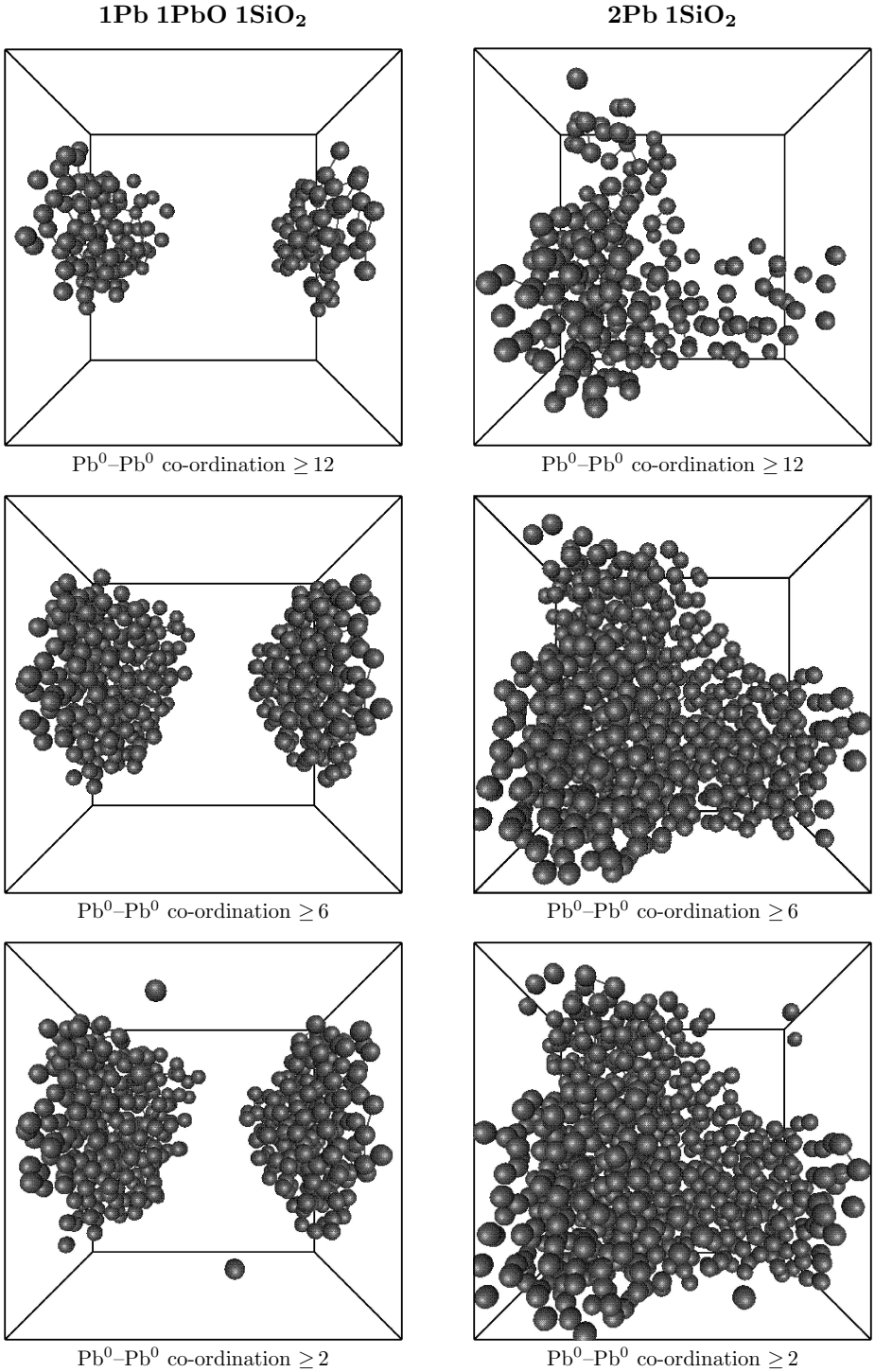

Figure 8. Pb^0 atom configurations in the last step of the sampling run at room temperature for the 1Pb 1PbO $1SiO_2$ and 2Pb $1SiO_2$ glasses (left, and right panels, respectively). The subsequent figures from top to bottom show all the Pb^0 atoms with Pb^0 co-ordinations equal or higher than 12, 6, and 2

Acknowledgements

The opportunity to perform our simulations at the TASK Computer Centre in Gdansk (Poland) is kindly acknowledged.

References

[1] Wang C C 1970 *Phys. Rev.* **B 2** 2045
[2] Wiza J L 1979 *Nucl. Instrum. Meth.* **62** 587
[3] Trzebiatowski K, Murawski L, Kościelska B, Chybicki M, Gzowski O and Davoli I 1997 *Proc. of the Conf. on Fundamentals of Glass Science and Technology*, Vaxjo, Sweden
[4] Warrel C A and Henshall T 1978 *J. Non-Cryst.Solids* **29** 283
[5] Verweij H and Konijnendijk W L 1976 *J. Am. Ceram. Soc.* **11-12** 517
[6] Zahra A M and Zahra C Y 1993 *J. Non-Cryst. Solids* **155** 45
[7] Fayon F, Bessada C, Massiot D, Farnan I and Coutures J P 1998 *J. Non-Cryst. Solids* **232-234** 403
[8] Fayon F, Landron C, Sakurai K, Bessada C and Massiot D 1999 *J. Non-Cryst. Solids* **243** 39
[9] Wang P W and Zhang L 1996 *J. Non-Cryst. Solids* **194** 129
[10] Morikawa H, Takagi Y and Ohno H 1982 *J. Non-Cryst. Solids* **53** 173
[11] Imaoka M, Hasegawa H and Yasui I 1986 *J. Non-Cryst. Solids* **85** 393
[12] Yamada K, Matsumoto A, Niimura N, Fukunaga T, Hayashi N and Watanabe N 1986 *J. Phys. Soc. Jap.* **55** 831
[13] Suzuya K, Price D L, Saboungi M-L and Ohno H 1997 *Nucl. Inst. Meth. Phys. Res.* **B 133** 57
[14] Masteraro V R, Zanotto E D, Lequeux N and Cortès R 2000 *J. Non-Cryst. Solids* **262** 191
[15] Witkowska A, Rybicki J, Trzebiatowski K, Di Cicco A and Minicucci M 1999 *Proc. 5th Int. Conf. on Intermolecular Interactions in Matter*, Lublin, p. 42
[16] Witkowska A, Rybicki J, Trzebiatowski K, Di Cicco A and Minicucci M 2000 *J. Non-Cryst. Solids* **276** 19
[17] Rybicki J, Rybicka A, Witkowska A, Bergmański G, Di Cicco A, Minicucci M and Mancini G 2001 *J. Phys. CM* **13** 9781
[18] Damodaran K V, Rao B G and Rao K J 1990 *Phys. Chem. Glasses* **31** 212
[19] Cormier G, Peres T and Capobianco J A 1996 *J. Non-Cryst. Solids* **195** 125
[20] Rybicki J, Alda W, Rybicka A and Feliziani S 1996 *Comp. Phys. Commun.* **97** 191
[21] Rybicka A, Chybicki M, Laskowski R, Alda W and Feliziani S 1997 *Proc. 4*$^{\text{th}}$ *Int. Conf. on Intermolecular Interaction in Matter*, Gdansk, p. 42
[22] Rybicka A 1999 *The Structure and Properties of Lead-silicate and Lead-germanate Glasses: a Molecular Dynamics Study,* PhD Thesis, Technical University of Gdansk, Gdansk
[23] Rybicka A, Rybicki J, Witkowska A, Feliziani S and Mancini G 1999 *Comput. Met. Sci. Technol.* **5** 67
[24] Hockney R W and Eastwood J W 1987 *Computer Simulation using Particles*, McGraw-Hill
[25] Rapaport D C 1995 *Art of the Molecular Dynamics Simulation*, University Press, Cambridge
[26] Filipponi A 1994 *J. Phys. CM* **6** 8415
[27] D'Angelo P, Di Nola A, Filipponi A, Pavel N V and Roccatano D 1994 *J. Chem. Phys.* **100** 985
[28] Filipponi A and Di Cicco A 1995 *Phys. Rev.* **B 51** 12322
[29] Brostow W, Chybicki M, Laskowski R and Rybicki J 1998 *Phys. Rev.* **B 57** 13448
[30] Laskowski R, Rybicki J and Chybicki M 1997 *TASK Quart.* **1** 96
[31] Laskowski R 2000 *TASK Quart.* **4** 531
[32] Rybicki J, Laskowski R and Feliziani S 1996 *Comp. Phys. Commun.* **97** 185
[33] Balducci R and Pearlman R S 1994 *J. Chem. Inf. Comput. Sci.* **34** 822
[34] Mancini G 1997 *TASK Quart.* **1** 89
[35] Mancini G 2001 *Comp. Phys. Commun.* **143** 187
[36] Bergmański G, Rybicki J and Mancini G 2000 *TASK Quart.* **4** 555
[37] Rybicki J, Bergmański G and Mancini G 2001 *J. Non-Cryst. Solids* **293-295** 758
[38] www.task.gda.pl/software
[39] Medvedev N N and Naberukhin Y I 1987 *J. Non-Cryst. Solids* **94** 402

[40] Elliott R 1995 *J. Non-Cryst. Solids* **182** 1
[41] Hamann D R 1997 *Phys. Rev.* **B 55** 14784
[42] Wyckoff R W G 1964 *Crystal Structures*, Wiley-Interscience Publications, New York